Matter and Radiation at Extremes | RESEARCH ARTICLE | scitation.org/journal/mre

Extreme matter compression caused by radiation cooling effect in gigabar shock wave driven by laser-accelerated fast electrons

Cite as: Matter Radiat. Extremes 6, 020301 (2021); doi: 10.1063/5.0026002
Submitted: 20 August 2020 • Accepted: 19 December 2020 •
Published Online: 25 January 2021

S. Yu. Gus'kov,[1] P. A. Kuchugov,[1,2,a)] and G. A. Vergunova[1]

AFFILIATIONS

[1]P. N. Lebedev Physical Institute of the Russian Academy of Sciences, Moscow, Russia
[2]Keldysh Institute of Applied Mathematics of the Russian Academy of Sciences, Moscow, Russia

[a)]**Author to whom correspondence should be addressed:** pkuchugov@gmail.com

ABSTRACT

Heating a solid material with laser-accelerated fast electrons is a particularly useful method for generating a plane powerful shock wave with a pressure of several hundred or even thousands of Mbar in the laboratory. Behind the front of such a powerful shock wave, dense plasma is heated to a temperature of several keV. Then, a high rate of radiation energy loss occurs even in low-Z plasmas. In this paper, the strong compression of matter due to radiation cooling in a Gbar shock wave driven by fast electrons is studied using both computational and theoretical approaches. It is shown that the effect of radiation cooling leads to compression of matter in the peripheral region of the shock wave to a density several times greater than the density at its front. Heating a solid material by a petawatt flux of laser-accelerated fast electrons offers the opportunity to surpass the gigabar pressure level of plane shock waves generated by the impact of laser-accelerated pellets. Higher pressures of about 100 Gbar can be achieved under laboratory conditions only when a spherical target is imploded under the action of a terawatt laser pulse.

I. INTRODUCTION

Heating a solid material with a laser-accelerated charged particle beam is an effective way to generate a powerful plane shock wave with a pressure of several hundred or even thousands of megabars (Mbar)[1–3] in a laboratory experiment. This is due to the fact that the energy flux density of such a beam is close to the intensity of the laser pulse that produces it. At the same time, in contrast to laser radiation, charged particles transmit their energy in Coulomb collisions and are thus able to heat a substance with a density that significantly exceeds the critical plasma density. The continual growth in the energies available at modern laser facilities with terawatt and petawatt power outputs allows us to consider laser-accelerated charged particle beams as an effective tool for generating the super-powerful shock waves in sufficiently large volumes of matter that meet the needs of such important applications as inertial confinement fusion (ICF), studies of the equations of state (EOS) of materials, and laboratory astrophysics. It should be noted that the above comments apply primarily to laser-accelerated electron beams, since the efficiency of laser energy conversion into fast electron energy is significantly (two to three times) larger than the efficiency of conversion into fast ion energy.

The potential capabilities of shock wave generation by heating a solid material with a petawatt flux of laser-accelerated fast electrons go beyond those of the method based on the impact of laser-accelerated pellets,[4,5] which has been shown to be capable of generating a plane shock wave with the record pressure of 740 Mbar.[4] This pressure is close to the maximum achievable with the impact method, since the collisional mechanism of laser radiation absorption is limited by the value of the coupling parameter $I\lambda^2 \approx 2 \times 10^{14}$ W μm^2/cm^2 (where I and λ are respectively the intensity and wavelength of the laser radiation). The record pressure was determined by the limiting intensity for the third Nd-laser harmonic of 10^{15} W/cm^2. The method based on direct heating of a solid material by laser-accelerated fast electrons is designed to use intensities exceeding the collisional absorption limit, for which a significant fraction of laser energy is transformed into the energy of fast electrons. It was shown in Ref. 6 that the use of a laser pulse with an intensity of $I \approx 10^{19}$ W/cm^2–10^{21} W/cm^2 to heat a solid by fast electrons can generate a plane shock wave with a pressure of several tens of gigabars (Gbar). Higher pressures of up to several hundred Gbar can be achieved in the laboratory only in the case when a spherical target is imploded under

the impact of a terawatt laser pulse. Therefore, in, for example, EOS studies, heating by laser-accelerated fast electrons offers great promise, bearing in mind the complicated diagnostic methods that are required when a spherical configuration is used compared with the traditional methods that can be applied in experiments with a plane shock wave.

This work is devoted to further study of the properties of shock waves driven by heating solid materials with laser-accelerated electron beams. In Ref. 6, it was shown that with this heating method, radiation energy loss is the main factor limiting the temperature of the plasma that is produced. In the compressed material behind the shock wave front, radiation energy loss plays an even greater role than in the heated region. The extreme compression of matter due to radiation cooling in a shock wave driven by laser-accelerated fast electrons is studied using both computational and theoretical approaches. This increase in compression due to radiation cooling is well known in the context of laminar flows in Z pinches[7–10] and in ICF target[10,11] implosions. It should be noted that the radiation cooling effect is a central problem in astrophysics and laboratory astrophysics, particularly in the context of accretion physics[12] and radiative laboratory shock physics.[13]

In this paper, the effect of radiation cooling behind the front of a powerful shock wave is considered. It is shown that this cooling leads to compression of matter in the peripheral region of the shock wave to a density several times greater than that at its front. First, in Sec. II, the features of the radiation cooling effect in a powerful shock wave driven by heating a dense material with laser-accelerated electrons are discussed. Then, in Sec. III, the results of numerical calculations are presented and discussed. Finally, Sec. IV presents the conclusions of the study.

II. FEATURES OF A SHOCK WAVE DRIVEN BY LASER-ACCELERATED FAST ELECTRONS

The generation and propagation of a shock wave driven by heating the boundary region of a half-space with a monoenergetic laser-accelerated fast electron flow are considered here. The dimensional parameters of the problem are the energy flux density of fast electrons I_h and the mass range of the heating particles in the heated substance μ_h, which is a function of the initial fast electron energy ε_h and the density of the substance ρ_0. According to numerous experimental results and theoretical models, the efficiency of laser energy conversion into fast electron energy, $\eta = I_h/I_L$, lies in the range 0.1–0.3. Despite this relatively low conversion efficiency, laser-accelerated electrons are the undisputed record holder for energy flux density among the charged particle beams that can be generated in the laboratory, taking into account the laser intensities of 10^{20} W/cm^2–10^{21} W/cm^2 that are currently available. The energy ε_h increases with laser intensity I_L and wavelength λ and can reach ultrarelativistic values. The dependence $\varepsilon_h(I_L, \lambda)$ is given by the following well-known scalings[14,15] based on data from numerous experiments and theoretical models:

$$\varepsilon_h\,[\mathrm{MeV}] = \begin{cases} 0.45\,(I_{L(19)}\lambda_\mu)^{1/3} & (I_{L(19)}\lambda_\mu^2 < 0.1), \\ 1.2\,(I_{L(19)}\lambda_\mu)^{1/2} & (I_{L(19)}\lambda_\mu^2 > 0.1), \end{cases} \tag{1}$$

where $I_{L(19)}$ and λ_μ are measured in units of 10^{19} W/cm^2 and μm, respectively.

The calculated results were obtained for the case of impact of laser irradiation on aluminum, which is often used as a reference material in EOS experiments. For estimates, the following approximation formulas are used for the mass ranges of nonrelativistic and relativistic electrons, which are based on the data from Refs. 2, 16, and 17 for an aluminum plasma with ionic charge $Z = 11$:

$$\mu_h\,[\mathrm{g/cm^2}] \approx \begin{cases} 0.8\varepsilon_h^2 & (\varepsilon_h < 1\ \mathrm{MeV}), \\ 0.9\varepsilon_h & (\varepsilon_h > 1\ \mathrm{MeV}), \end{cases} \tag{2}$$

where the energy ε_h is measured in units of MeV.

The scales of the physical quantities in the problem are determined by the thermodynamic parameters of a region heated by fast electrons. In plane geometry, the mass of the heated layer remains constant and equal to the fast electron mass range, despite the increase in the temperature of the heated layer and the decrease in its density due to thermal expansion. Under these conditions, the thermodynamic state of the heated layer is described by the solutions obtained in Ref. 1. For the period of quasistatic heating, when the motion of the substance can be ignored, these solutions are

$$\rho = \rho_0, \quad T = T_h\frac{t}{t_h}, \quad P = P_h\frac{t}{t_h} \quad (0 \le t \le t_h), \tag{3}$$

and for the subsequent period of thermal expansion of the layer with a constant mass, they are

$$\rho = \rho_0\left(\frac{t_h}{t}\right)^{3/2}, \quad T = T_h\frac{t}{t_h}, \quad P = P_h\left(\frac{t_h}{t}\right)^{1/2} \quad (t \ge t_h). \tag{4}$$

In these expressions, t_h is the duration of the quasistatic heating period or the time of ablation loading (following the notation of Ref. 1), during which an isothermal rarefaction wave propagates from the outer surface of the half-space to the inner boundary of the heated layer:

$$t_h \equiv \frac{\mu_h}{2\rho_0 c_T} = \frac{1}{2}\left[\frac{9}{2(\gamma-1)}\right]^{1/3}\frac{\mu_h}{\rho_0^{2/3} I_h^{1/3}}. \tag{5}$$

Here, μ_h is the mass range of an electron with energy ε_h, and $c_T = [C_V(\gamma-1)T_h]^{1/2}$ is the isothermal sound speed in the heated region, where $C_V = (Z+1)k_B/[A(\gamma-1)m_p]$ is the specific heat at constant volume, k_B is Boltzmann's constant, m_p is the proton mass, A and Z are the atomic number and ionic charge, and γ is the specific heat ratio. In the expressions (3) and (4), T_h and P_h are the temperature and pressure that are reached at the end of the quasistatic heating period and are given by

$$T_h = \frac{1}{C_V}\left[\frac{9}{16(\gamma-1)}\right]^{1/3}\left(\frac{I_h}{\rho_0}\right)^{2/3}, \qquad P_h = \left[\frac{3(\gamma-1)}{4}\right]^{-2/3}\rho_0\left(\frac{I_h}{\rho_0}\right)^{2/3}, \tag{6}$$

where I_h is the flux energy density of fast electrons.

Using the expressions (1) and (2) for the energy and the mass range of fast electrons, it is easy to find that the characteristic time of thermodynamic state evolution t_h increases with both the laser intensity and wavelength. In the nonrelativistic case, t_h grows as $t_h \sim I_L^{1/3}\lambda^{4/3}$, and in the relativistic case, it grows as $t_h \sim I_L^{1/6}\lambda$. In the

case of an aluminum plasma at $I_L = 10^{18}$ W/cm^2, with $\lambda = 1.06$ μm (the first harmonic of the Nd laser), which corresponds to $\varepsilon_h = 200$ keV, and at a conversion efficiency $\eta = 0.2$, the ablation loading time is about 130 ps.

From the point of view of achieving an extreme state of matter, the most interesting period is the initial one of shock wave propagation, when quasistatic heating occurs. Then, the properties of the shock wave can be determined under the approximation of a uniform pressure distribution in the heated region and in the region brought into motion by the shock wave. Then, the shock wave velocity D_{SW} and the temperature T_{SW} behind the shock wave front can be expressed in terms of the thermodynamic parameters of the heated region as follows:

$$D_{SW} \approx \left(\frac{\gamma+1}{2}\right)^{1/2} c_T,$$
$$T_{SW} \approx \frac{P_h}{C_V \rho_{SW}} = \frac{\gamma-1}{\gamma+1} T_h. \quad (7)$$

The scales of pressure P_h and temperature T_h during the quasistatic heating depend only on the flux heating energy density I_h and are independent of the heating particle energy ε_h. This is a fundamental difference between material heating and shock wave generation driven by a charged particle beam and those driven by a laser pulse. The pressure and temperature of a laser-heated material depend on the energy of a light quantum through the critical plasma density ρ_{cr}, which is the scale of density in the region of absorption of radiation with the given quantum energy:[18,19] $T_L \sim (I_L/\rho_{cr})^{2/3}$ and $P_L \sim \rho_{cr}^{1/3} I_L^{2/3}$ (where $\rho_{cr} \approx 1.83\times10^{-3} A/Z\lambda_\mu^2$ g/cm^3, with λ_μ being the laser radiation wavelength measured in units of μm).

At the same values of I_h and I_L, in comparison with the case of laser heating, the pressure of plasma heated by fast electrons is larger by a factor of approximately $(\rho_0/\rho_{cr})^{1/3}$, while the temperature, by contrast, is smaller by a factor of $(\rho_0/\rho_{cr})^{2/3}$. However, in a shock wave, the temperature ratio is reversed. Indeed, in the approximation of a uniform distribution of pressure, the ratio of temperatures in shock waves driven by fast electrons and laser radiation is $T_{SW(h)}/T_{SW(L)} = P_h/P_L = (\rho_0/\rho_{cr})^{1/3}$. The temperature in a shock wave driven by a powerful laser pulse is, as usual, several tens of eV, whereas the temperature in a shock wave driven by a fast electron beam can reach a value of several keV. Such a high temperature is a distinctive feature of shock waves driven by fast electrons. Generation of shock waves with Gbar pressure and keV temperature is a record opportunity for a laboratory experiment. This high temperature of a dense plasma is the reason for the intense bremsstrahlung emission and the associated increase in compression of matter in the transparent plasma of the shock wave. Thermal conduction occurs at the ablation boundary (in the region of the shock wave piston) and has almost no smoothing effect in the shock wave region. Thus, the conditions are favorable for radiation cooling and, as a result, for increased compression of matter in the shock wave. Simple estimates relating to the quasistatic heating confirm this. The averaged mean free path of thermal radiation in the region involved with the shock wave can be estimated as[20]

$$l_r = \frac{4\sigma T^4}{W_r}, \quad (8)$$

where $\sigma = 1.03 \times 10^{17}$ J cm^{-2} s^{-1} keV^{-4} is the Stefan–Boltzmann constant, and W_r is the emissivity of plasma electrons,[20] given by

$$W_r\,[\mathrm{Jcm^{-3}\,s^{-1}}] = 1.73 \times 10^{17} \left(\frac{Z}{A}\right)^2 Z T^{1/2} \rho^2, \quad (9)$$

where the temperature T and density ρ are measured in units of keV and g/cm^3, respectively.

Below, an example is considered that corresponds to irradiation of an aluminum target with first-harmonic Nd-laser radiation with an intensity of 10^{18} W/cm^2 ($\varepsilon_h = 200$ keV) at a conversion efficiency $\eta = 0.2$, which corresponds to a fast electron energy flux density of 2×10^{17} W/cm^2. According to (2), the mass range of fast electrons with energy 200 keV in an aluminum plasma with charge $Z = 11$ is about 0.032 g/cm^2. Further, according to (5)–(7) at $\gamma = 5/3$, the duration t_h of quasistatic heating and the average temperature for this period behind the shock wave front are about 130 ps and 1.5 keV. Substituting $T = 1.5$ keV, $\rho \approx 4\rho_0 = 10.8$ g/cm^3, and $Z = 11$ into (8) and (9), we obtain a value of $l_r \approx 0.03$ cm for the radiation mean free path, which is about 10 times larger than the size of the shock wave region, $l_{SW} = D_{SW} t_h \approx 0.004$ cm. Then, for the example under consideration, the flux energy density of the thermal radiation carried away, $q_r = W_r l_{SW}$, is about of 10^{17} W/cm^2, which is half the fast electron energy flux density. In the approximation of adiabatic compression of the matter in the radiation-cooled region, the increase in density in this region compared with the density at the shock wave front can be estimated as

$$\frac{\rho}{\rho_{SW(0)}} \approx \left(1 - \frac{q_r}{q_h}\right)^{-1/(\gamma-1)}, \quad (10)$$

where $\rho_{SW(0)} = \rho_0(\gamma+1)/(\gamma-1)$. For $q_r/q_h = 0.5$, this estimate gives an excess density in the radiation-cooled region compared with the density at the shock wave front of about 2.8. This means that a density of about 30 g/cm^3 can be achieved in an aluminum target.

There now follows a discussion of plasma heating by a beam of laser-accelerated fast electrons from the point of view of the establishment of the thermodynamic state of the resulting plasma. For a deceleration length of a subrelativistic fast electron of about 100 μm–200 μm, the time taken for its energy to be transferred to plasma electrons is about 1 ps. This is much shorter than the hydrodynamic time of the problem, which is about 100 ps–200 ps, and thus a fast electron transfers its energy to the plasma with stationary distributions of thermodynamic parameters. In turn, the energy transfer time is much longer than the plasma relaxation times, i.e., the electron–electron and electron–ion energy relaxation times, which for a plasma density in the heating region of several g/cm^3 and a temperature of several keV are 0.0001 ps and 0.1 ps, respectively. The collisional ionization time is about 0.001 ps and involves the participation of plasma electrons with a Maxwellian spectrum. The main recombination mechanism under the conditions of the problem under consideration is triple collision. The recombination rate in a triple collision exceeds the photorecombination rate by more than 100 times, which means that a Saha equilibrium in terms of the ionization composition is established. Thus, heating of the material by laser-accelerated fast electrons occurs while the local thermodynamic equilibrium of the plasma is maintained.

III. NUMERICAL RESULTS AND DISCUSSION

The bulk of numerical calculations were performed using the one-dimensional two-temperature hydrodynamic code DIANA,[21] supplemented by a module of energy transfer by fast electrons.[22] The

DIANA code takes into account all the main relaxation and transport processes in the plasma and the real equations of state. The energy transfer by intrinsic plasma radiation is considered under the approximation of volumetric losses due to the bremsstrahlung mechanism. The cooling function operates through a threshold frequency for photons: all photons with frequency above the threshold value leave the plasma and take away their energy, while for photons with frequency below the threshold, the energy is deposited locally. This code has been used successfully in investigations of the effect of energy transfer by fast electrons on the gain of direct-drive ICF targets.[22,23] The energy transfer from fast electrons in Coulomb collisions is calculated using a model of the stopping power of the plasma electrons adjusted for scattering by the plasma ions.[2,16,17] The controlling calculations were performed using the RADIAN numerical code,[24,25] which solves the one-dimensional equations of two-temperature gas dynamics together with the radiation transfer equation. When solving the radiative transfer equation, this code uses the multigroup approximation, the method of characteristics, the quasidiffusion method, and averaging over photon energies to effectively reduce the dimensions of the equation. These calculations showed that taking radiation transfer into account led to insignificant deviations of the thermodynamic parameters at a level of 5%–10% from the DIANA code results. Calculations using the DIANA code were performed in the range of fast electron energy flux density $I_h = 2 \times 10^{16}$ W/cm^2 -2×10^{19} W/cm^2, which, with the supposed efficiency of laser energy conversion into fast electron energy of $\eta = 0.2$, corresponds to a range of variation in laser intensity of $I_L = 10^{17}$ W/cm^2–10^{20} W/cm^2. The initial energy of fast electrons was chosen according to the scaling (1) for the first harmonic of the Nd-laser radiation, and varied from a nonrelativistic energy $\varepsilon_h = 100$ keV to a relativistic energy $\varepsilon_h = 3.8$ MeV.

Figures 1–3 show the results of a numerical calculation of shock wave propagation in aluminum under a fast electron energy flux density of $I_h = 2 \times 10^{17}$ W/cm^2 and an initial energy $\varepsilon_h = 200$ keV (which corresponds to an intensity of the first harmonic of Nd-laser radiation $I_L = 10^{18}$ W/cm^2 at a conversion efficiency $\eta = 0.2$). The mass range of fast electrons with the energy indicated above is about $\mu_h \approx 0.028$ g/cm^2. The mass range varies slightly with increasing temperature and decreasing density in the heated region, in accordance with the change in the Coulomb logarithm. Figure 1 shows the distributions of pressure, electron temperature, and density over the mass coordinate from the boundary of the half-space, on which the source of fast electrons was set, to the shock wave front at different moments in time. The mass coordinates of the edge of the half-space and the inner boundary of the heated region are respectively 0.54 g/cm^2 and about 0.512 g/cm^2. The time evolution of the thermodynamic parameter distributions is shown in the region heated by fast electrons and the shock wave region. The pressure has a fairly uniform distribution behind the front of the shock wave. Moreover, it varies nonmonotonically with time. From the initial time, the pressure behind the shock wave front reaches a value of about 10 Gbar at about 120 ps, after which it decreases to a minimum of about 6.5 Gbar at about 200 ps, then increases again, reaching a second maximum of about 7.5 Gbar at about 500 ps, and further decreases monotonically. The temperature distribution has a minimum and the density distribution has a maximum in the peripheral region of the shock wave, the positions of which fall at the same value of the mass coordinate. The maximum density in the radiation-cooled region reaches a value of about 45 g/cm^3 at about 500 ps.

Figure 2 shows the time dependences of the numerically calculated values of the maximum pressure and maximum density, together with the time dependence of the pressure in the heated region, calculated on the basis of the analytical solutions (3)–(6) with a fraction of radiation energy loss of 40%. In the initial period up to 120 ps–150 ps, when the initial stage of shock wave formation occurs, the maximum pressure is determined by the pressure in the heated region. The solution (3) for the stage of quasistatic heating is in good agreement with the numerically calculated dependence. The pressure increases with time in a nearly linear manner and reaches a value of about 10 Gbar by a time of about 130 ps–150 ps. The ablation loading time t_h is about 150 ps, and the maximum value of the numerically calculated pressure is reached at $t = 130$ ps. During the ablation loading period, the temperature behind the shock wave is about 1 keV and the length of shock wave propagation is about 0.002 cm. The corresponding averaged mean free path of thermal photons is 0.01 cm, which is five times greater than the length of shock wave propagation. All of these values are in good agreement with the estimates in Sec. II, made on the basis of the expressions (3)–(9). As a result, the whole shock wave is transparent, and the growth in density begins from the wave front and reaches its maximum in the peripheral back region. At subsequent moments in time, the shock wave propagates under conditions of expansion of the heated region as a whole and ablation of matter at a depth exceeding the mass range of fast electrons. This minimizes the numerically calculated pressure dependence at $t = 180$ ps. The steady motion of the shock wave ends at a time of about 400 ps, after which the pressure decreases monotonically with time. The pressure in the steady-state shock wave is 30%–40% higher than the pressure from the analytical solution (4) in the heated region, which is a consequence of hydrodynamic energy transfer to a substance of higher density. At the end of the period of steady-state movement of the shock wave, the maximum value of the density is reached in its peripheral part. Subsequently, the maximum density decreases in accordance with the decrease in pressure.

Figure 3 shows the profiles of pressure, density, electron temperature, and plasma emissivity at $t = 500$ ps, corresponding to the attainment of maximum density values in the peripheral part of the shock wave. An increase in density in the peripheral region of the shock wave occurs near the maximum value of the plasma emissivity. The maximum compression to a density of 45 g/cm^3 occurs in the region that is cooled to the maximum extent owing to radiation energy losses under the action of the maximum pressure developed in the shock wave. The degree of compression due to radiation cooling increases with laser pulse intensity, owing to increases both in pressure and in radiation energy loss. In the calculation for impact of radiation of the first harmonic of the Nd laser with intensity $I_L = 10^{19}$ W/cm^2 ($\varepsilon_h = 1.2$ MeV) and a conversion efficiency from laser energy to fast electron energy of $\eta = 0.2$, the maximum density reaches a value of 65 g/cm^3.

Numerical simulations conducted for a Cu target show an increase in the maximum density in the peripheral area of the shock wave compared with the result for an aluminum target. In the case of impact of a laser beam of intensity 10^{18} W/cm^2 ($\varepsilon_h = 200$ keV and $\eta = 0.2$), the maximum density reaches a value of about 58 g/cm^3, whereas for a laser intensity 10^{19} W/cm^2 and a particle energy of

1.2 MeV, it reaches a value of 66 g/cm^3. The saturation of the increase in density in the peripheral region of the shock wave with an increase in atomic number is associated with saturation of the increase in radiation energy losses: the increase in emissivity is compensated by a decrease in the transparency of the radiation region. In particular, in the numerical simulation of a Cu target with a laser intensity of 10^{18} W/cm^2, the time of ablation loading t_h is about 60 ps and the temperature T_h is about 0.5 keV. Both of these values are approximately half of those obtained from the calculations for an Al target, in accordance with (4) and (5). The corresponding averaged mean free path of thermal photons l_r in the Cu plasma, with its density approximately three times that of the Al plasma, is about 0.000 06 cm. During the period of ablation loading, the length of shock wave propagation is about 0.0005 cm, which is eight times larger than l_r. So, in contrast to the case of an Al target, where all of the shock wave is transparent and the growth in density begins from the wave front and reaches its maximum in the peripheral back region, the main part of the shock wave in Cu target is opaque, and a growth in density occurs only in the narrow peripheral region. It should be noted that to achieve higher densities, the intensity of the fast electron flux needs to

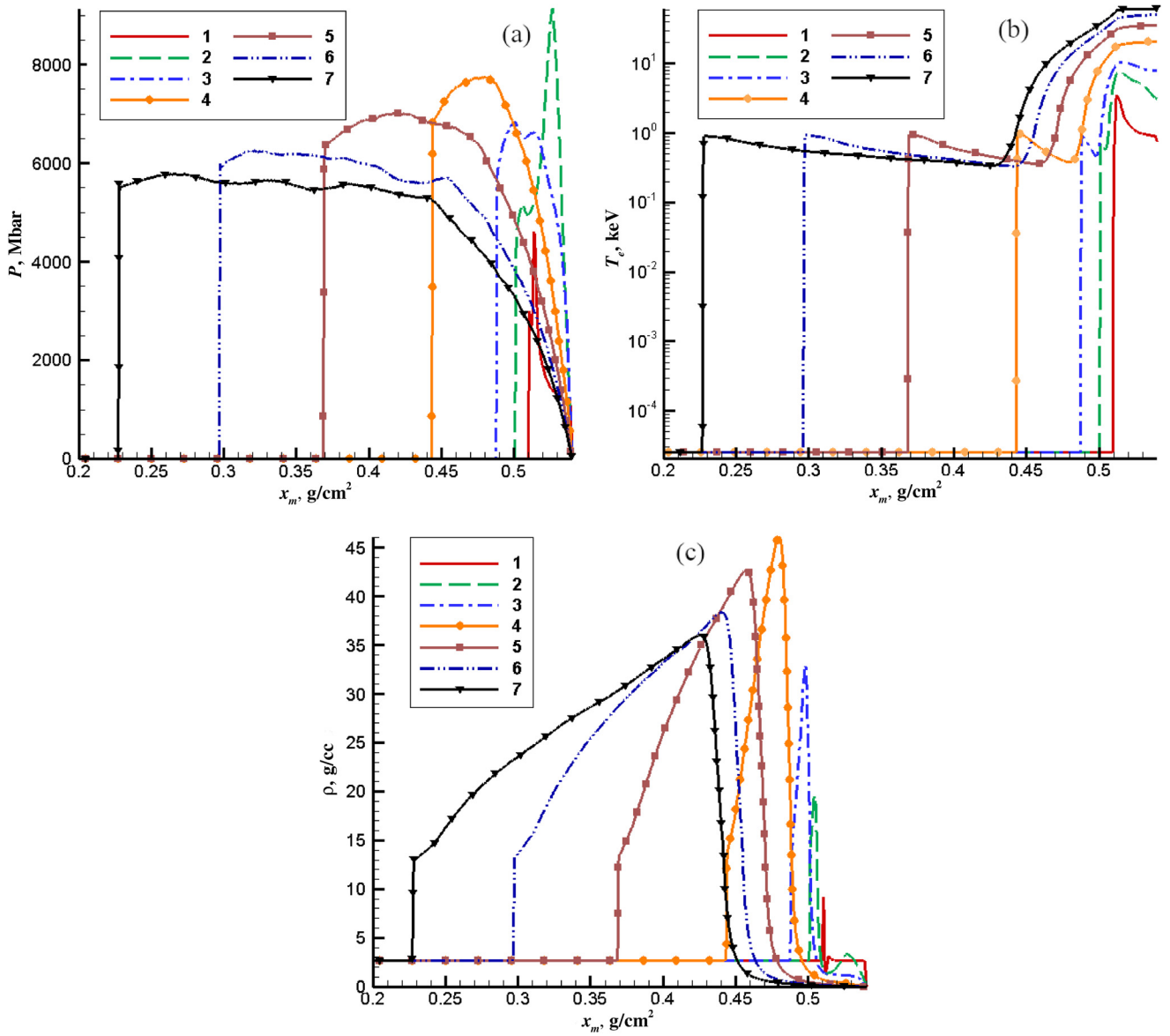

FIG. 1. Profiles of (a) pressure, (b) electron temperature, and (c) density over the mass coordinate at various moments in time: 20 ps (curves 1), 100 ps (curves 2), 200 ps (curves 3), 500 ps (curves 4), 1 ns (curves 5), 1.5 ns (curves 6), and 2 ns (curves 7). These results were obtained from calculations for the impact of fast electrons with energy flux density $I_h = 2 \times 10^{17}$ W/cm^2 and initial energy $\varepsilon_h = 200$ keV.

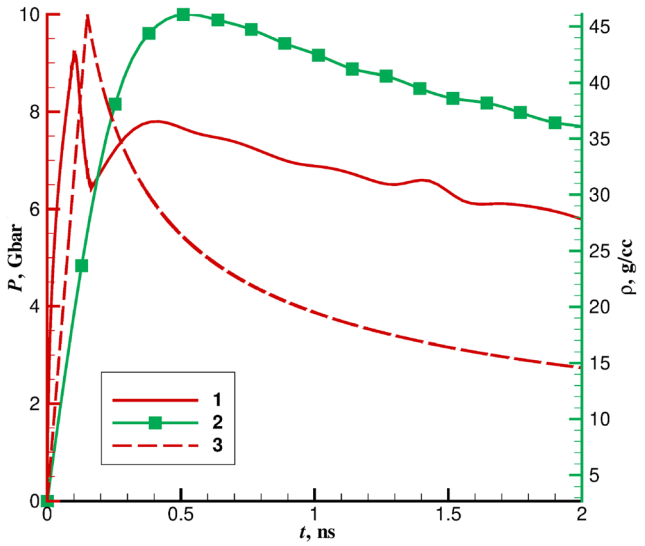

FIG. 2. Time dependences of the numerically calculated maximum values of pressure (curve 1) and density (curve 2), together with the pressure in the heated region according to the analytical expressions (3)–(6) under the impact of fast electrons with energy flux density $I_h = 2 \times 10^{17}$ W/cm^2 and initial energy $\varepsilon_h = 200$ keV.

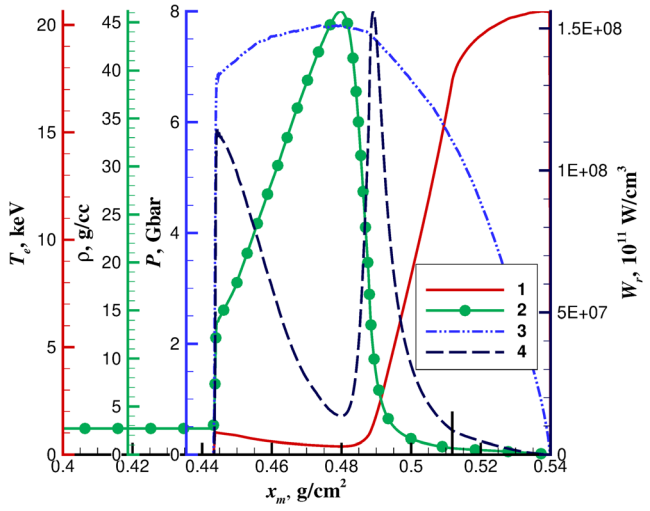

FIG. 3. Profiles of electron temperature (curve 1), density (curve 2), pressure (curve 3), and plasma emissivity (curve 4) at a moment in time 500 ps, which corresponds to the attainment of maximum density in the peripheral region of the shock wave. These data were obtained from calculations for the impact of fast electrons with energy flux density $I_h = 2 \times 10^{17}$ W/cm^2 and initial energy $\varepsilon_h = 200$ keV. The short vertical line indicates the inner boundary of the heated region.

be increased while the initial energies of the particles are kept the same. This has not yet been achieved in current experiments, although there is now the possibility of using laser acceleration as a powerful source of fast electrons.

The calculation results that have been presented here allow one to determine the experimental conditions for EOS studies. For a laser pulse with an intensity of 10^{18} W/cm^2, the pulse duration corresponding to the maximum density values is about 100 ps. To generate a nearly plane shock wave, the radius of the laser beam must be at least two lengths of thermal expansion of the heating region, i.e., about 100 μm. This means that the energy of the laser pulse in this case should be about 4 kJ–5 kJ.

Shock waves generated by heating solid materials using fast electrons may be of interest for laboratory studies of the physics of radiative shocks. The generation of such waves is due to the work done by a dense, high-temperature piston. As a result, a stratified strongly collisional plasma structure is formed (with a Coulomb logarithm of about 10), with inhomogeneous distributions of thermodynamic parameters. The region of strong radiation, located in the peripheral region of the shock wave at the interface with the piston, is relatively narrow, with a mass that does not exceed 10% of the mass of the piston. Electron thermal conductivity has a negligible effect on the thermodynamic state of this region. The radiation region, in the form of a plasma structure created by heating, is largely transparent to radiation. The optical thickness of the region heated by fast electrons (the high-temperature piston) is 0.0001. The optical thickness in the region of strong radiation is about 0.1 for mid-Z materials such as Al and about 0.5 for high-Z materials such as Cu. However, the optical thickness in the entire region covered by the shock wave can vary from fractions of unity for mid-Z materials up to several multiples of unity for high-Z materials. In the conditions of the problem under consideration, the Péclet number with respect to the electron thermal conductivity (the ratio of the hydrodynamic velocity to the velocity of the wave front of electron heat conduction) for the radiation region is quite large for both Al and Cu targets, with values of about 200–300. The Péclet number with respect to radiation is different for different regions of the stratified plasma structure. In the region of strong radiation, its value is about 10^6 for an Al target and 10^5 for a Cu target. The cooling parameter (the ratio of cooling time to hydrodynamic time) is about 0.01 for mid-Z materials and about 0.1 for high-Z ones. Plasma structures with such properties, created by heating a material with a petawatt flux of laser-accelerated fast electrons, are of likely interest with regard to laboratory astrophysics in connection with the effect of radiation cooling as controlled by changes in the laser pulse intensity and by appropriate selection of the target material.

IV. CONCLUSION

Heating a solid material with a beam of laser-accelerated fast electrons can generate shock waves with properties particularly suitable for laboratory experiments. The pressure behind the front of such a shock wave can reach several hundreds and even thousands of Mbar at a temperature of several keV. Such a high temperature causes a high rate of radiation energy loss in a dense plasma, which is then partially transparent to intrinsic radiation. As a result, the conditions arise for strong radiation cooling and consequently increased plasma compression in the peripheral part of the shock wave. The theoretical and computational studies reported here show that under the impact of radiation of the first harmonic of a Nd laser with intensity 10^{17} W/cm^2–10^{19} W/cm^2, the density of an aluminum plasma in the peripheral region of a fast-electron-driven shock wave can reach 30 g/cm^3–60 g/cm^3, while a density of 50 g/cm^3–70 g/cm^3 can be reached for a copper plasma. With an increase in the atomic

number of the irradiated material, saturation of the increase in density occurs in the peripheral region of the shock wave, which is associated with saturation of the growth of radiation energy losses, where the increase in emissivity is compensated by a decrease in the transparency of the radiation region. This approach offers the possibility of investigating the states of materials at pressures of several Gbar, temperatures of several keV, and densities of several tens of g/cm^3 and thus represents a new avenue for laboratory studies of material EOS. Investigation of the increase in density in the peripheral region of the shock wave, which is determined by radiative energy losses, is of great interest for establishing the optical properties of materials with high atomic number. In addition, the dependence of the increase in density on the degree of ionization makes it possible to study the kinetics of ionization of matter at ultrahigh pressures, which is a topic of great importance for physics at high energy densities. Such experiments can be performed using a sub-nanosecond laser pulse with an energy of 1 kJ–10 kJ.

REFERENCES

[1]S. Gus'kov, X. Ribeyre, M. Touati, J.-L. Feugeas, P. Nicolaï, and V. Tikhonchuk, "Ablation pressure driven by an energetic electron beam in a dense plasma," Phys. Rev. Lett. **109**, 255004 (2012).

[2]X. Ribeyre, S. Gus'kov, J.-L. Feugeas, P. Nicolaï, and V. T. Tikhonchuk, "Dense plasma heating and Gbar shock formation by a high intensity flux of energetic electrons," Phys. Plasmas **20**, 062705 (2013).

[3]S. Y. Gus'kov, "On the possibility of laboratory shock wave studies of the equation of state of a material at gigabar pressures with beams of laser-accelerated particles," JETP Lett. **100**, 71–74 (2014).

[4]R. Cauble, D. W. Phillion, T. J. Hoover, N. C. Holmes, J. D. Kilkenny, and R. W. Lee, "Demonstration of 0.75 Gbar planar shocks in x-ray driven colliding foils," Phys. Rev. Lett. **70**, 2102–2105 (1993).

[5]M. Karasik, J. L. Weaver, Y. Aglitskiy, T. Watari, Y. Arikawa, T. Sakaiya, J. Oh, A. L. Velikovich, S. T. Zalesak, J. W. Bates, S. P. Obenschain, A. J. Schmitt, M. Murakami, and H. Azechi, "Acceleration to high velocities and heating by impact using Nike KrF laser," Phys. Plasmas **17**, 056317 (2010).

[6]S. Y. Gus'kov, N. P. Zaretskii, and P. A. Kuchugov, "Features and limiting characteristics of the heating of a substance by a laser-accelerated fast electron beam," JETP Lett. **111**, 135–138 (2020).

[7]R. S. Pease, "Equilibrium characteristics of a pinched gas discharge cooled by bremsstrahlung radiation," Proc. Phys. Soc., Sect. B **70**, 11–23 (1957).

[8]V. V. Vikhrev, "Contraction of Z-pinch as a result of losses to radiation," JETP Lett **27**(2), 95–98 (1978).

[9]L. Bernal and H. Bruzzone, "Radiative collapses in z-pinches with axial mass losses," Plasma Phys. Controlled Fusion **44**, 95–98 (2002).

[10]R. S. Craxton, K. S. Anderson, T. R. Boehly, V. N. Goncharov, D. R. Harding, J. P. Knauer, R. L. McCrory, P. W. McKenty, D. D. Meyerhofer, J. F. Myatt, A. J. Schmitt, J. D. Sethian, R. W. Short, S. Skupsky, W. Theobald, W. L. Kruer, K. Tanaka, R. Betti, T. J. B. Collins, J. A. Delettrez, S. X. Hu, J. A. Marozas, A. V. Maximov, D. T. Michel, P. B. Radha, S. P. Regan, T. C. Sangster, W. Seka, A. A. Solodov, J. M. Soures, C. Stoeckl, and J. D. Zuegel, "Direct-drive inertial confinement fusion: A review," Phys. Plasmas **22**, 110501 (2015).

[11]I. E. Golovkin, J. J. MacFarlane, P. R. Woodruff, J. E. Bailey, G. Rochau, K. Peterson, T. A. Mehlhorn, and R. C. Mancini, "Spectroscopic analysis and NLTE radiative cooling effects in ICF capsule implosions with mid- dopants," J. Quant. Spectrosc. Radiat. Transfer **99**, 199–208 (2006).

[12]J. M. Blondin and D. F. Cioffi, "The growth of density perturbations in radiative shocks," Astrophys. J. **345**, 853 (1989).

[13]J. Laming, "Relationship between oscillatory thermal instability and dynamical thin-shell overstability of radiative shocks," Phys. Rev. E **70**, 057402 (2004).

[14]F. N. Beg, A. R. Bell, A. E. Dangor, C. N. Danson, A. P. Fews, M. E. Glinsky, B. A. Hammel, P. Lee, P. A. Norreys, and M. Tatarakis, "A study of picosecond laser–solid interactions up to 10^{19} w cm^{-2}," Phys. Plasmas **4**, 447–457 (1997).

[15]M. G. Haines, M. S. Wei, F. N. Beg, and R. B. Stephens, "Hot-electron temperature and laser-light absorption in fast ignition," Phys. Rev. Lett. **102**, 045008 (2009).

[16]S. Atzeni, A. Schiavi, and J. R. Davies, "Stopping and scattering of relativistic electron beams in dense plasmas and requirements for fast ignition," Plasma Phys. Controlled Fusion **51**, 015016 (2008).

[17]J. J. Honrubia and J. Meyer-ter-Vehn, "Three-dimensional fast electron transport for ignition-scale inertial fusion capsules," Nucl. Fusion **46**(11), L25–L28 (2006).

[18]Y. V. Afanasiev and S. Y. Gus'kov, "Energy transfer to the plasma in laser targets," in *Nuclear Fusion by Inertial Confinement: A Comprehensive Treatise* (CRC Press, 1993), pp. 99–119.

[19]J. Lindl, "Development of the indirect-drive approach to inertial confinement fusion and the target physics basis for ignition and gain," Phys. Plasmas **2**, 3933–4024 (1995).

[20]Y. B. Zel'dovich and Y. P. Raizer, in *Physics of Shock Waves and High-Temperature Hydrodynamic Phenomena*, edited by W. D. Hayes and R. F. Probstein (Academic Press, 1967).

[21]N. V. Zmitrenko, V. Y. Karpov, A. P. Fadeev, I. I. Shelaputin, and G. V. Shpatakovskaya, "Description of the physical processes in the DIANA program for calculations of problems of laser fusion," Ser. Methods Software Numer. Solution Probl. Math. Phys. **2**(13), 34–37 (1983).

[22]S. Y. Gus'kov, P. A. Kuchugov, R. A. Yakhin, and N. V. Zmitrenko, "Effect of 'wandering' and other features of energy transfer by fast electrons in a direct-drive inertial confinement fusion target," Plasma Phys. Controlled Fusion **61**, 055003 (2019).

[23]S. Y. Gus'kov, P. A. Kuchugov, R. A. Yakhin, and N. V. Zmitrenko, "Effect of fast electrons on the gain of a direct-drive laser fusion target," Plasma Phys. Controlled Fusion **61**, 105014 (2019).

[24]G. A. Vergunova and V. B. Rozanov, "Influence of intrinsic X-ray emission on the processes in low-density laser targets," Laser Part. Beams **17**, 579–583 (1999).

[25]V. B. Rozanov and G. A. Vergunova, "Investigation of compression of indirect-drive targets under conditions of the NIF facility using one-dimensional modelling," Quantum Electron. **50**, 162–168 (2020).